Diffusion Hydrodynamic Model Shallow Estuary

By G. L. Guymon,[1] Fellow, ASCE, M. N. Khan,[2] M. Collins,[3] and T. V. Hromadka,[4] Member, ASCE

ABSTRACT: Many of the hydrodynamic models used for estuary tidal flows and storm surges are based on a set of coupled two-dimensional hydrodynamic equations, which are obtained from the full three-dimensional flow equations by averaging the vertical coordinates. Various numerical techniques, such as finite difference, finite element, and the method of characteristics, have been used to solve these equations. The diffusion hydrodynamic model (DHM) has been developed to simulate two-dimensional surface-water and channelized flows. In a prior study, the DHM was applied to a deep-water estuary with computational results, comparable to those obtained using the St. Venant equations and the method of characteristics. In this paper, the DHM is applied to a shallow estuary located in southern California. The main objective is to determine local flow velocities and circulation patterns in the shallow estuary caused by the incoming and the outgoing tide. Verification of the DHM is provided by comparison of tidal gage measurements and computed flow depths.

INTRODUCTION

The diffusion hydrodynamic model (DHM) (Hromadka and Yen 1986) has been applied to several applications, including dam-break flood analysis (Guymon and Hromadka 1986), river overflow floodplain analysis (Hromadka et al. 1989), and other hydrodynamic problems. In this paper, the DHM is extended to accommodate use of irregularly shaped finite element four-sided polygons. The extended DHM is then applied to a shallow estuary in order to simulate water surfaces and flow velocities. This extension marks *the first use of irregularly shaped polygons in the DHM. In the shallow* estuary problem, tidal gage measurements are collected as data for comparison to the computed DHM results, providing for partial calibration and verification.

Detail is also paid toward computational efficiency issues in the DHM. A variable time-step scheme is employed where time-step sizes used in the time-advancement algorithm are increased or decreased according to the success in meeting prescribed incremental changes in computed flow depths. Use of a predictor-corrector technique in estimating the time-step size reduces the number of iterations needed to advance the solution vector in time.

DESCRIPTION OF STUDY REGION

Newport Bay and its watershed are located in south central Orange County, Calif., about 72 km (45 mi) south of Los Angeles, the largest city in southern

[1]Prof., Dept. of Civ. Engrg., Univ. of California, Irvine, CA 92717.
[2]Grad. Student, Univ. of Calif., Irvine, CA.
[3]Grad. Student, Univ. of Calif., Irvine, CA.
[4]Prof., Dept. of Mathematics, California State Univ., Fullerton, CA 92634.

Ca.   .nia. The watershed includes the cities of Costa Mesa, Newport Beach, Irvine, Santa Ana, Orange, Tustin, and unincorporated areas of Orange County. The catchment area encompasses about 388 sq km (150 sq mi) (Fig. 1).

Newport Bay is a shallow estuary with a mean water surface area of about 4.9 sq km (1.9 sq mi) and about 37 km (23 mi) of shoreline. It is T-shaped, extending along the coast about 6 km (4 mi), separated from the Pacific Ocean by a narrow split called "Newport Peninsula." This "lower" area includes six islands and is the most heavily developed portion of the bay. The bay shores are completely developed with residential and commercial uses and there are numerous docks where pleasure boats are moored. This area of the bay receives intensive recreational use throughout the year. The lower bay is connected to the Pacific Ocean by a man-made jetty on its southeastern edge near the community of Corona Del Mar, a portion of the city of Newport Beach.

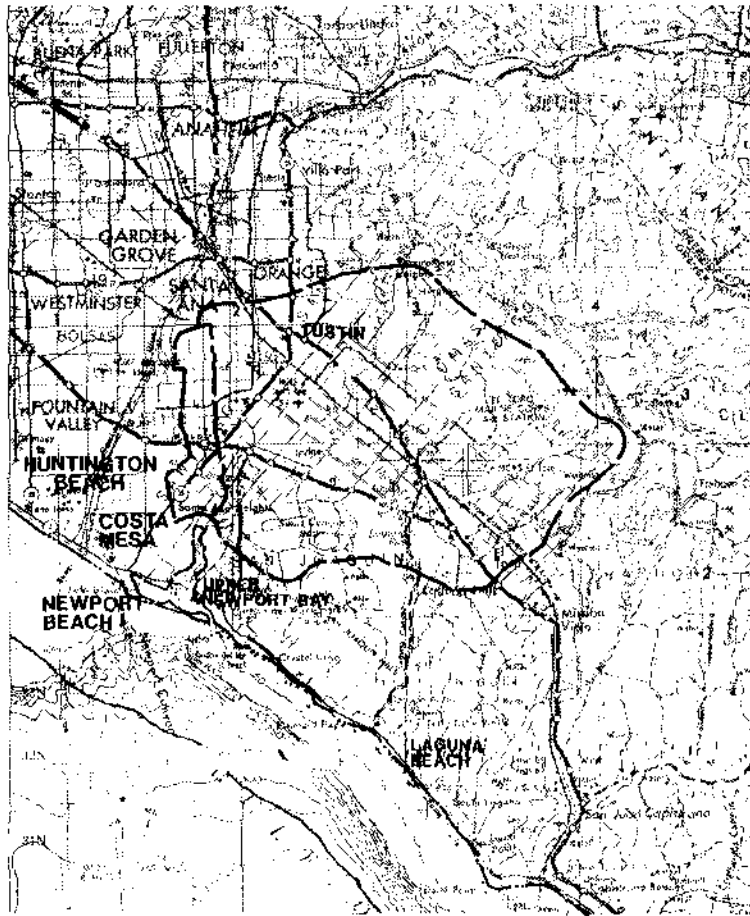The "leg" of the T-shaped bay extends inland toward the north about 4

mi. This portion of the bay is characterized by shallower   .er and tidal effects that expose extensive mud flats during low tides. Surrounding bluffs are developed, but the shore areas are natural. In the most upper part of the "upper bay" (back bay), there is a state ecological preserve managed by the State Department of Fish and Game. This area, in particular, is a habitat for numerous water fowl, birds, and other small animals. The upper bay area is heavily vegetated by salt marsh vegetation, typical to southern Calif. lagoons and estuaries.

A composite bottom contour map is shown in Fig. 2. Contours and shore areas depicted reflect 1986 conditions and use mean lowest low water (MLLW) as data. Contour elevations range between about 20 ft below MLLW in the jetty at the Pacific Ocean to over 1 m (4 ft) above MLLW in a number of areas in the uppermost reaches of the upper bay. Wetted areas fluctuate with the tides.

Newport Bay is subject to a shallow but complex tidal cycle characteristic of the southern California bight. Two low and two high tides occur diurnally and are particularly pronounced during the highest tides during the new moon phase of the lunar cycle. The two tides are less noticeable during the full-moon phase of the lunar cycle when tides are lowest. As is shown

FIG. 1.   Newport Bay, San Diego Creek, and Santa Ana Delhi Channel Watersheds

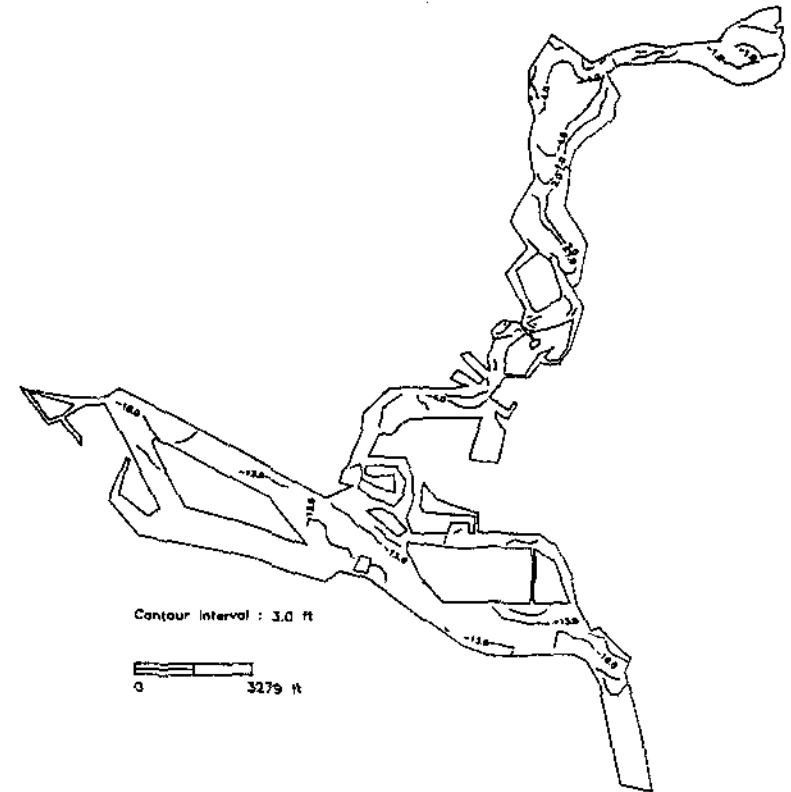Contour Interval : 3.0 ft

0   3279 ft

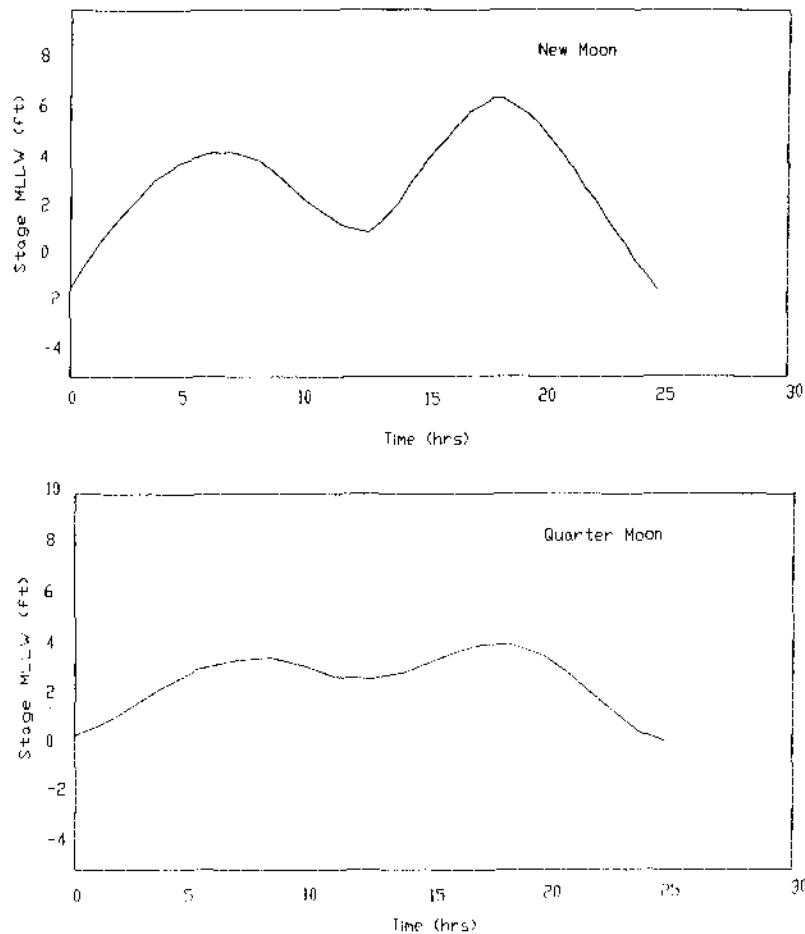FIG. 2.   Newport Bay, Contours of Bottom Elevation

FIG. 3. Typical Diurnal Tidal Cycles for New-Moon and Quarter-Moon Conditions at NOAA Newport Bay Gage

subsequently, tides are propagated rapidly throughout the bay system. Fig. 3 depicts a typical new-moon tide and quarter-moon tide during a diurnal cycle.

Two major streams and 23 minor streams or storm drains are tributary to Newport Bay. The largest tributary stream is San Diego Creek, with 313 sq km (121 sq mi) of drainage area. Flows in the San Diego Creek channel have ranged from a summer base flow of about 0.71 m³/s (25.2 cfs) to a peak value of 439 m³/s (15,500 cfs), recorded during the storm of March 1, 1983. Mean flows are about 1.37 m³/s (48.5 cfs). The Santa Ana Delhi channel, the second largest stream tributary of the bay, drains about 4,662 ha (18 sq mi) principally in the valley floodplain. Flows in the Santa Ana Delhi channel tributary to the bay have ranged from a low base flow of 0.1 m³/s (3.4 cfs) to a peak value of 123 m³/s (4,346 cfs) recorded during the storm of March 1, 1983. Mean flows are about 0.25 m³/s (8.8 cfs).

MATHEMATICAL MODEL DEVELOPMENT

Numerous investigators have developed hydrodynamic models that could be applied to the Newport Bay estuary. Early in this investigation it was decided that a two-dimensional flow model would be required but such a model must be simplified, eliminating some of the processes found in complete models to achieve computation speed. Such a modeling approach is provided by the diffusion hydrodynamic model (DHM) as reported by Akan and Yen (1981), Hromadka et al. (1985), Guymon and Hromadka (1986), Hromadka and Yen (1986), DeVries et al. (1986), and Hromadka et al. (1988, 1989).

Because of the estuary's shallowness relative to its aerial extent, little loss in precision in describing currents will occur if the water column is considered as vertically integrated; thus, a two-dimensional model in the aerial plane will be sufficient. Complete hydrodynamic equations of fluid motion in an open body of water are developed by considering conservation of mass and momentum. First, consider a square finite volume, or cell, in a flow field; conservation of mass or continuity is given by

$$\frac{\partial q_x}{\partial_x} + \frac{\partial q_y}{\partial y} + \frac{\partial h}{\partial t} = 0 \quad \dots\dots\dots\dots\dots\dots\dots\dots\dots (1)$$

where x, y = horizontal coordinates; t = time; q_x and q_y = discharge per unit length perpendicular to the indicated direction; and h = mean water column depth. Conservation of momentum is expressed in terms of the St. Venant equations

$$\frac{\partial Q_x}{\partial t} + \frac{Q_x}{A_x} \frac{\partial Q_x}{\partial x} + \frac{Q_y}{A_x} \frac{\partial Q_x}{\partial y} + gA_x \left(S_{f_x} + \frac{\partial H}{\partial x} \right) = 0 \quad \dots\dots\dots (2)$$

$$\frac{\partial Q_y}{\partial t} + \frac{Q_x}{A_y} \frac{\partial Q_y}{\partial x} + \frac{Q_y}{A_y} \frac{\partial Q_y}{\partial y} + gA_y \left(S_{f_y} + \frac{\partial H}{\partial y} \right) = 0 \quad \dots\dots\dots (3)$$

where Q_x and Q_y = total discharge across a cell face in the indicated directions; A_x and A_y = cross-sectional areas of the cell face; g = gravitational constant; S_{f_x} and S_{f_y} = friction slopes in the indicated directions due to bottom shear only; and $H = h + z$ (z = height of the water column invert alone above an arbitrary horizontal datum). For a small bay like Newport Bay, Coriolis effects may be assumed to be negligible. Discharge (Q) may be linked to friction slope (S_f) by Manning's equation for normal depth flow

$$Q_i = \frac{1.486}{n} A_i R_i^{2/3} S_{f_i}^{1/2} \quad \dots\dots\dots\dots\dots\dots\dots\dots\dots (4)$$

where $i = x, y$ (British units are used); n = Manning's invert roughness coefficient; and R = hydraulic radius. For wide shallow channels $R \approx h$.

Referring to the aforementioned St. Venant equations, the first term is the local acceleration term and the second two terms are the inertial terms. Hromadka et al. (1985), Guymon and Hromadka (1986), and Hromadka and Yen (1986) have shown that for relatively shallow flows where velocities are relatively small, these terms may be neglected without undue loss of precision. Consequently, the St. Venant equations reduce to

$$S_{f_i} = \frac{\partial H}{\partial X_i} \quad \cdots\cdots (5)$$

where $i = x, y$. Then Manning's equation may be rearranged as

$$Q_i = -K_i \frac{\partial H}{\partial X_i} \quad \cdots\cdots (6)$$

where

$$K_i = \frac{1.486}{n} b_i h_i^{5/3} \Big/ \left|\frac{\partial H}{\partial X_i}\right|^{1/2} \quad \cdots\cdots (7)$$

with $i = x, y$.

This result may be substituted into the flow continuity equation (1) to yield the so-called diffusion hydrodynamic equation in two-dimensions

$$\frac{\partial}{\partial x}\left(K_x \frac{\partial H}{\partial x}\right) + \frac{\partial}{\partial y}\left(K_y \frac{\partial H}{\partial y}\right) = A_{x,y} \frac{\partial h}{\partial t} \quad \cdots\cdots (8)$$

where $A_{x,y}$ = aerial area of the cell. This equation is a parabolic equation (diffusion equation) that is highly nonlinear because K function of water level gradient and depth. Consequently, only numerical solutions are possible. A straightforward finite difference approximation of (8), by reconsidering the continuity equation, is as follows: instead of writing this equation in terms of q, we write it in terms of total discharge Q, by

$$\frac{\partial Q_x}{\partial x} \Delta x + \frac{\partial Q_y}{\partial y} \Delta y = A_{x,y} \frac{\partial h}{\partial t} \quad \cdots\cdots (9)$$

Integrating the partial-differential components

$$\Delta Q_x + \Delta Q_y = A_{x,y} \frac{\Delta h}{\Delta t} \quad \cdots\cdots (10)$$

or, in an explicit solution scheme for any shaped cell

$$h^{J+1} = h^J + \frac{\Delta t}{A_{x,y}} \sum_i Q_i \quad \cdots\cdots (11)$$

where J = time step number; Q_i = discharge across a perpendicular cell face, being positive if inflow and negative if outflow; and Q_i and velocities are determined from

$$Q_i = -K_i \frac{\partial H}{\partial X_i} \quad \cdots\cdots (12)$$

where K_i is determined from (7). In the K_i equation, the h_i and $\partial H/\partial X_i$ terms may be computed by iterating with respect to the half-time step, or some other scheme. To reduce iteration, a tolerance in nodal value changes is set by requiring

$$\max|H^{J+1} - H^J| < \varepsilon_1 \quad \cdots\cdots (13)$$

where the maximum variation of all cells are scanned to determine if an ε_1 is exceeded. If it is, the time step is reduced in size and H^{J+1} recomputed or, if the step is much less, the time step is increased. Modeling applications

in this study indicate that a good value for ε_1 is 0.1. A slightly different criteria may also be used for the selection of the time step. This may be defined as

$$\max\left|\frac{H^{J+1} - H^J}{H^J}\right| < \varepsilon_2 \quad \cdots\cdots (14)$$

A value of 0.1 for ε_2 is a sufficient condition for the study. Note that the most sensitive location for the criteria varies with time and is different for the two different definitions. Hence, a third criteria, a combination of the two tolerances, may be used to test the shift of sensitivity of the solution from one criteria to the other. It has been determined that with the prescribed values of ε_1 and ε_2, the criteria for the absolute difference in head dominates in the selection of the time step. Further study of this time step corrector method is under way. We have also found that the time step changes as a function of simulation time, and can be fit to a spline curve (which is application dependent) such that Δt can be predicted beforehand, avoiding iteration.

To solve the explicit hydrodynamic equation algorithm just presented, initial conditions and boundary conditions are required. Initial conditions are of little importance since within a few hours (real-time) in most solutions
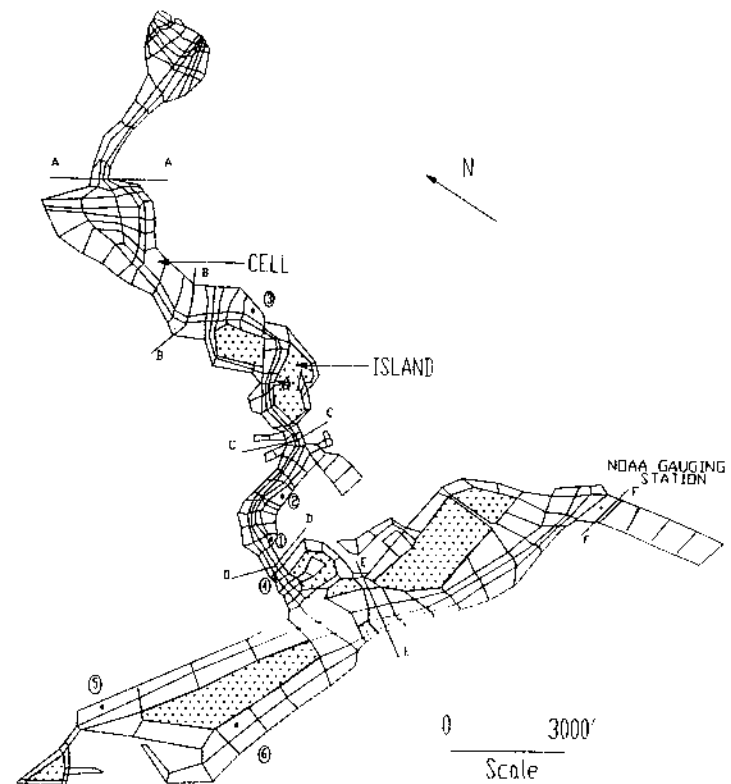

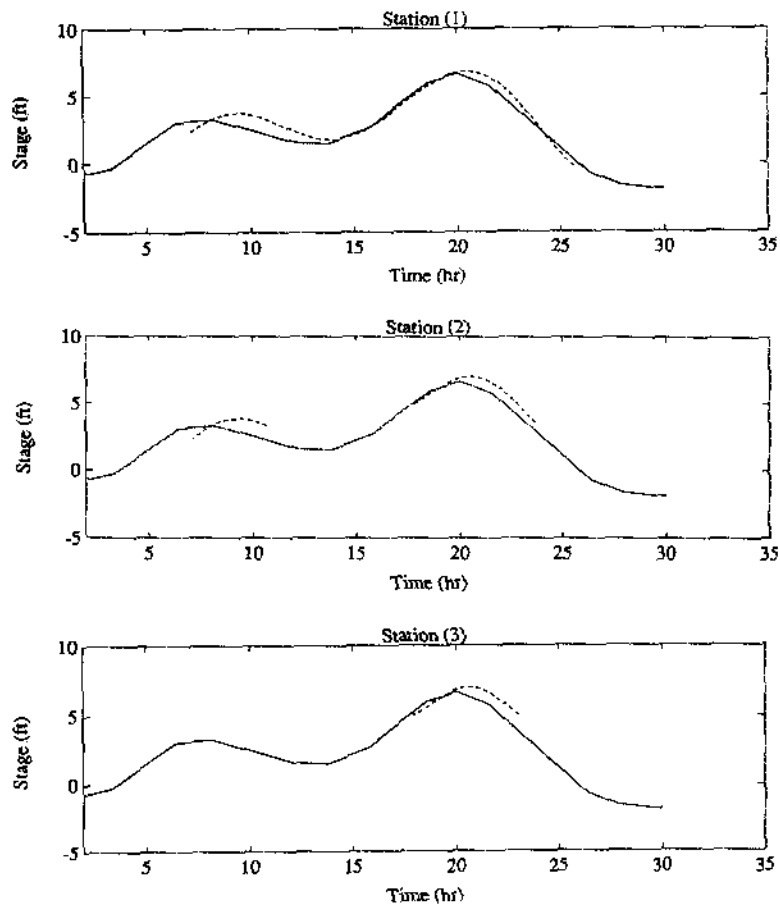FIG. 4. Newport Bay, Mathematical Model Grid

FIG. 5. Upper Newport Bay Measured Water Surface Elevations Compared to NOAA Gage (Solid Line), May 24–25, 1990

FIG. 6. Lower Newport Bay Measured Water Surface Elevations Compared to NOAA Gage (Solid Line), May 24–25, 1990

the initial condition effects die out. Consequently, the simulation will commence with a flat bay water surface at MLLW.

Two types of boundary conditions are considered in this model. One tidal boundary condition will be specified at the jetty-ocean mouth based upon the National Oceanic and Atmospheric Administration (NOAA) tidal gage located at the Harbor Master headquarters compound about 0.25 mi inside the bay from the jetty-ocean mouth. Tidal data input is of the form shown in Fig. 3 and intermediate tidal levels to these specified data are linearly interpolated.

The second kind of boundary conditions consists of inflow hydrographs from 25 different tributary watersheds, which are determined based upon the Orange County "Hydrology Manual" and related procedures described by Bedient and Huber (1989). This kind of boundary condition is not utilized in this paper and its description will be deferred to a subsequent paper.
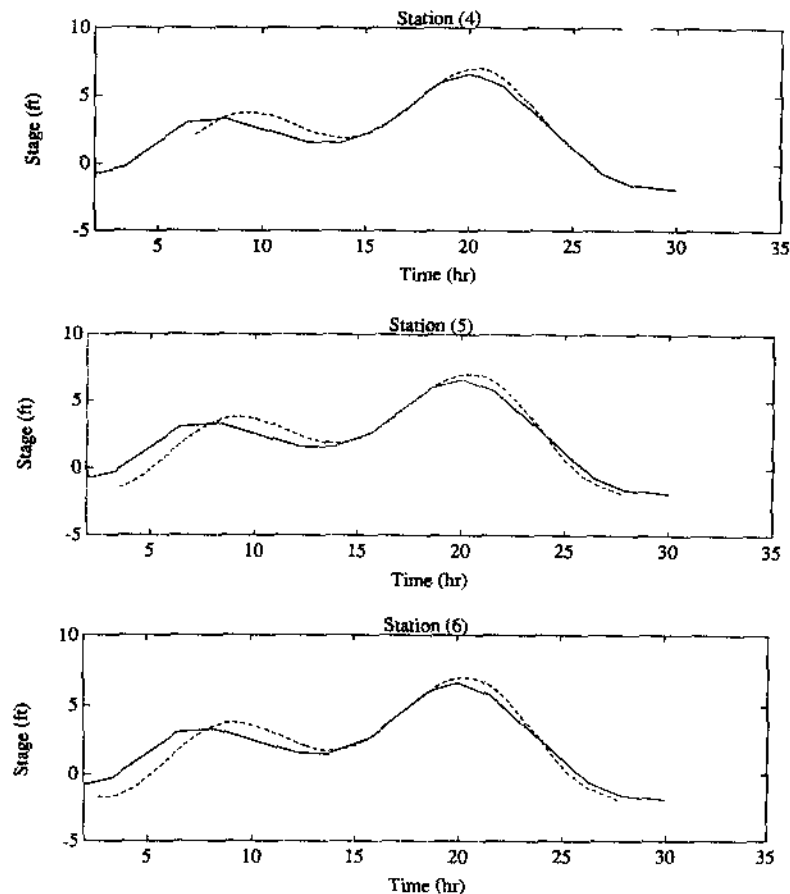
TABLE 1. Initial Manning's n-Factors for Newport Bay Hydrodynamic Model

Section (from Fig. 4) (1)	n-Factor (2)
A to B	0.015
B to C	0.030
C to D	0.045
D to E	0.030
E to F	0.020

DISCRETIZATION OF BAY

To solve the numerical hydrodynamic equation analog, the bay is discretized into quadrilateral finite elements. Generally, the greater the accuracy desired the more cells have to be defined. Furthermore, cells must be linked
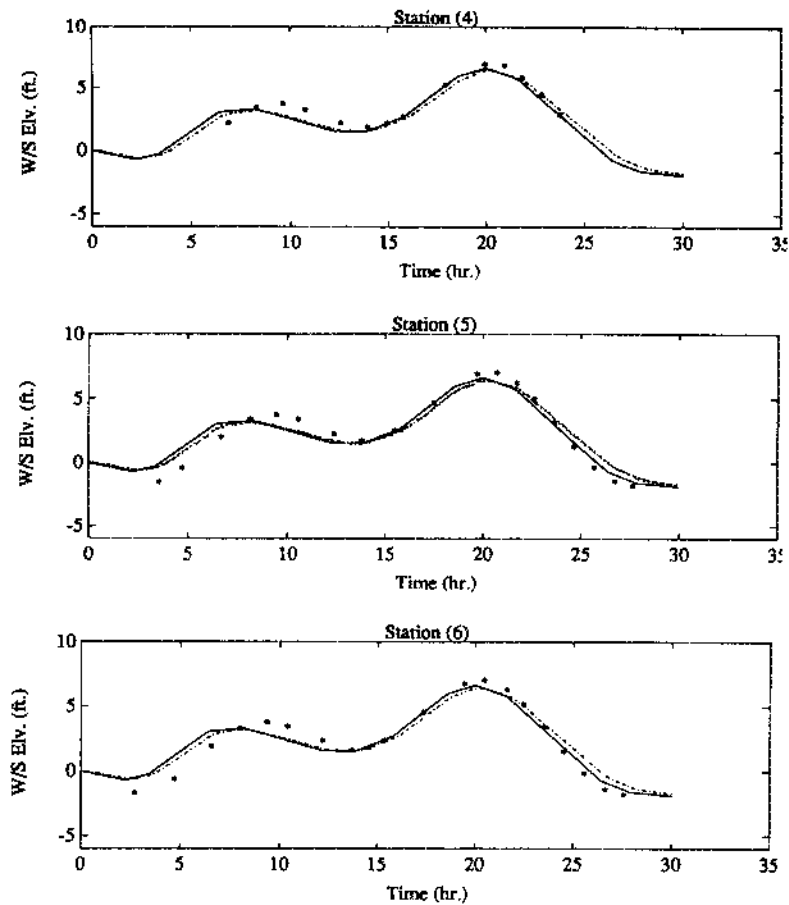
FIG. 7. Lower Newport Bay Comparison of Simulated Tides (Dashed Line) to Measured Tides (Asterisks) (NOAA Gage-Solid Line)

FIG. 8. Upper Newport Bay, Comparison of Simulated Tides (Dashed Line) to Measured Tides (Asterisks) (NOAA Gage-Solid Line)

in a continuous sense throughout the bay; however, islands are permissible. Several criteria were used to discretize the bay. To minimize simulation time, irregular cells were chosen because of the complex geometry of the bay. Because the ultimate objective of the model is to provide a tool for water-quality studies, water-quality data for the bay were reviewed and used to locate model nodal points. The discretization scheme selected is shown in Fig. 4. There are 395 cells and 549 nodes in the finite element system. Each cell and node is numbered in a systematic fashion. This scheme facilitates computational algorithms that determine cell face lengths normal to flow, cell volumes, and locating cells that are adjacent to each other in order to determine flow across boundaries. Each node requires coordinate data and bottom elevation data, which were determined from USGS 7.5 minute topographic quadrangle maps and the bathymetry map described previously. Cell numbers are used to identify tributary watershed points and the tidal boundary condition point.
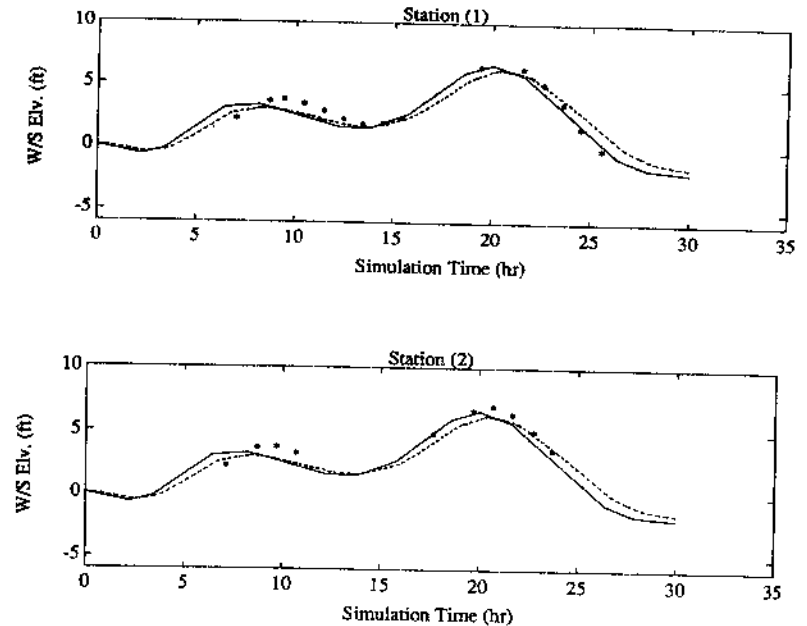
DHM MODEL VERIFICATION AND CALIBRATION

Because of the nonlinear nature of equations of fluid motion in the bay and its irregular geometry, closed forms of solutions are impossible, and there is no way to analytically determine the validity of the DHM computer program. The best one can do in this regard is to hold the K-values constant and solve the DHM equations analytically for a regular geometry and check for code errors. A limited amount of effort was conducted along these lines to ensure all portions of the code did not contain logic errors. In particular, severe shocks represented by short-duration high-amplitude tides were applied to simulated open water bodies to determine if the solutions were stable. Additionally, flooding of open rectangular tanks were simulated with good results.

The primary verification approach taken in this investigation was to measure a tidal sequence in several discrete portions of the bay and compare these data to simulated tides. Because the Manning's n-factor for bottom roughness must be assumed from experience, this approach is actually a partial verification and calibration effort combined. Partial verification is achieved in the sense that n-factors for each cell must be "tuned" to give good results and we must use judgment to determine if such tuning is realistic and the simulated tides and currents are reasonable.

Water surface elevations were measured at six locations (Fig. 4) in the bay over a 24-hr tidal diurnal cycle during May 24–25, 1990. This period, 5 A.M. on the 24th to 6 A.M. on the 26th, corresponded to maximum new-
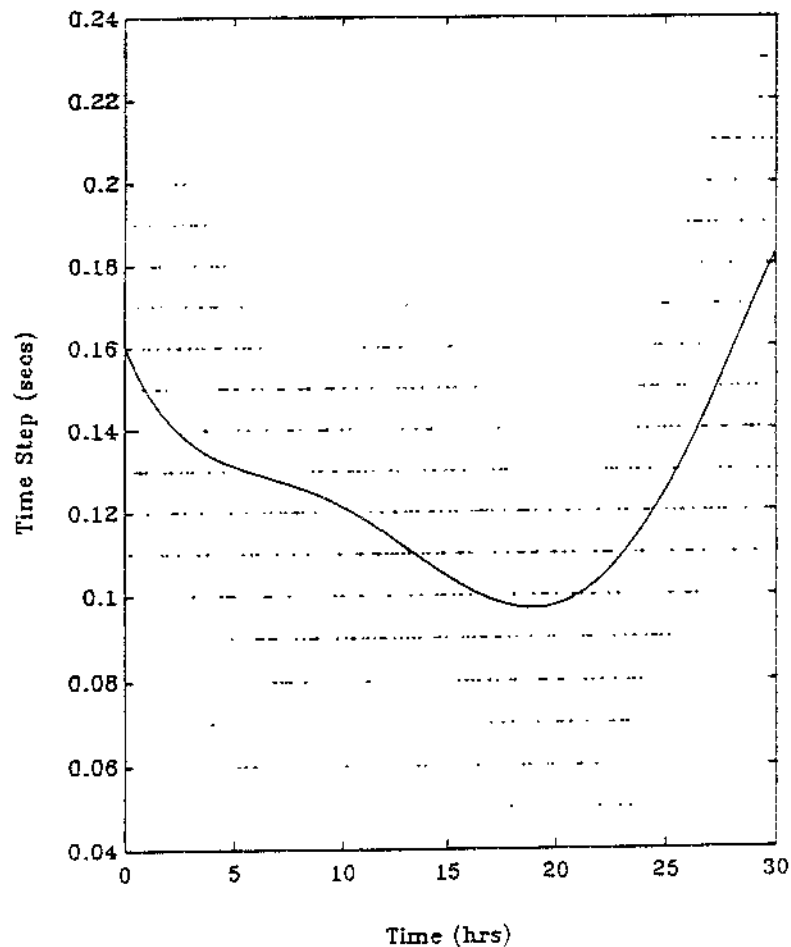
FIG. 9. Solution Time Step Size versus Simulated Clock Time and Spline Fit

moon tides during the lunar cycle. Measured tidal elevations at the NOAA tide gage were used as a boundary condition at the jetty mouth and minor tributary inflow during this period were neglected.

Tidal measuring stations were selected on the basis of proximity to Orange County benchmarks, and ease and safety in obtaining water level measurements. A temporary benchmark was surveyed for each measurement point and water levels were measured from the temporary benchmark down to the water surface. Teams of observers were organized to rotate throughout the 24-h period. Generally, water surfaces were measured on hourly intervals. The resulting tidal measurements are plotted in Figs. 5 and 6.

Calibration of the model to the measured tidal data was achieved by simulating tides and currents throughout the bay using the NOAA tidal data as the only boundary condition. The discretized geometry that approximates the bay geometry is assumed to be accurate. Manning's n-factors for bottom roughness are assumed and are the only parameters requiring

tuning. Table 1 presents the calibrated Manning's n-fac   or different sections of the bay.

Results are shown in Figs. 7 and 8, which compare measured tides to simulated tides at five locations. The actual tidal measuring sequence began at 5 A.M. To simulate measured tides a pseudotide was simulated for the previous 5 hr to remove the assumed bay water surface elevations initial conditions effects. As can be seen, the general shape of simulated stages closely approximate measured stages. Unfortunately, the datum of the NOAA gage seem to be somewhat different than the country surveyors datum and the chart time may be somewhat in error. Notice that the measured tides are larger in amplitude than the NOAA data.

Although currents were not measured as part of the verification effort, simulated currents appear reasonable. They are close to measured currents obtained several years ago as a test of a node-link model. Previous efforts to assess the accuracy of DHM model are discussed in Hromadka and Yen (1986, 1987). In the latter paper, the DHM approach was compared to a method of characteristics solution with good results.

During the various simulations and tests, considerable effort was expended in gaining insight into the solution characteristics. To achieve stable simulation with a minimum of local solution noise, time steps that were automatically determined by the code ranged from a minimum of about 0.05 to a maximum of about 0.22. Fig. 9 shows these times and shows a spline fit of the time step Δt, versus simulated clock time function. Usual time steps average 0.14 s. Using such a function to predetermine time steps materially speeds the execution time.

CONCLUSIONS

A diffusion hydrodynamic model (DHM) of a shallow estuary has been developed using an extension of the USGS DHM computer model (Hromadka et al. 1989). The DHM analog includes several hundred irregular polygon control volumes and nodal points. Simulation of estuary flow depths by the DHM analog were compared to measured tidal gage flow depths, with good agreement. Because the shallow estuary flow characteristics are two dimensional, a partial verification of the DHM is provided by the comparisons between tidal gage measurements and flow depths.

It must be noted that the DHM will only determine large scale circulation patterns. The method cannot determine small scale circulation or eddy phenomenon, which is important where water quality models are contemplated. The ultimate objective of this work is to develop water quality models and it is proposed that secondary small scale circulation be approximated by a dispersion parameter in the mass transport equation.

APPENDIX. REFERENCES

Akan, A. O., and Yen, B. C. (1981). "Diffusion-wave flood routing in channel networks." *J. Hydr. Div.*, ASCE, 107(6), 719–732.

nt, P. B., and Huber, W. C. (1989) *Hydrology and floodplain analysis*. Addison-Wesley, 650.

Guymon, G. L., and Hromadka, T. V. II. (1986). "Two-dimensional diffusion-probabilistic model of a slow dam break." *Water Resour. Bull.*, 22(2), 257–265.

Hromadka, T. V. II, Berenbrock, C. E., Freckleton, J. R., and Guymon, G. L. (1985). "A two-dimensional dam-break floodplain model." *Adv. Water Resour.*, 8, 7–14.

Hromadka, T. V. II, and Yen, C. C. (1986). "A diffusion hydrodynamic model (DHM)." *Adv. Water Resour.*, 9, 118–170.

DeVries, J. J., Hromadka, T. V. II, and Nestlinger, A. J. (1986). "Application of a two-dimensional diffusion hydrodynamic model." *Proc., HYDROSOFT*. CMl Publications, Southampton, England. 393–412.

Hromadka, T. V. II, Walker, T. R., and Yen, C. C. (1988). "Using the diffusion hydrodynamic model (DHM) to evaluate flood plain environmental impacts." *Envir. Software*, 3(1), 9–11.

Hromadka, T. V. II, Walker, T. R., Yen, C. C., and DeVries, J. J. (1989). "Application of the USGS diffusion hydrodynamic model for urban floodplain analysis." *Water Resour. Bull.*, 25(5), 1063–1071.